Physical-chemical mechanisms of pattern formation during gastrulation

Behnaz Bozorgui, Anatoly B. Kolomeisky, and Hamid Teimouri

Citation: The Journal of Chemical Physics **148**, 123302 (2018); doi: 10.1063/1.4993879
View online: https://doi.org/10.1063/1.4993879
View Table of Contents: http://aip.scitation.org/toc/jcp/148/12
Published by the American Institute of Physics

Physical-chemical mechanisms of pattern formation during gastrulation

Behnaz Bozorgui,[1] Anatoly B. Kolomeisky,[1] and Hamid Teimouri[2]
[1]*Department of Chemistry and Center for Theoretical Biological Physics, Rice University, Houston, Texas 77005-1892, USA*
[2]*Department of Physics and FAS Center for Systems Biology, Harvard University, Cambridge, Massachusetts 02138, USA*

(Received 2 July 2017; accepted 9 August 2017; published online 21 September 2017)

Gastrulation is a fundamental phase during the biological development of most animals when a single layer of identical embryo cells is transformed into a three-layer structure, from which the organs start to develop. Despite a remarkable progress in quantifying the gastrulation processes, molecular mechanisms of these processes remain not well understood. Here we theoretically investigate early spatial patterning in a geometrically confined colony of embryonic stem cells. Using a reaction-diffusion model, a role of Bone-Morphogenetic Protein 4 (BMP4) signaling pathway in gastrulation is specifically analyzed. Our results show that for slow diffusion rates of BMP4 molecules, a new length scale appears, which is independent of the size of the system. This length scale separates the central region of the colony with uniform low concentrations of BMP molecules from the region near the colony edge where the concentration of signaling molecules is elevated. The roles of different components of the signaling pathway are also explained. Theoretical results are consistent with recent *in vitro* experiments, providing microscopic explanations for some features of early embryonic spatial patterning. Physical-chemical mechanisms of these processes are discussed. *Published by AIP Publishing.* https://doi.org/10.1063/1.4993879

I. INTRODUCTION

Animals exhibit sophisticated body architectures that are established during the development when embryo cells extensively divide, differentiate, and migrate.[1–5] A critical stage of the development is gastrulation, which is a series of events that starts to transform the early embryos into a complex multilayered organism. During this phase, a single layer of originally nearly identical embryonic stem cells (ESCs) differentiates into three different germ layers of cells in an ordered spatial sequence.[1,2,5] A significant progress in delineating and quantifying the gastrulation processes has been achieved.[5,6] However, our understanding of the underlying molecular mechanisms of signaling and spatial pattern formation during the development remains quite limited.[4,5,7–10]

One of the most powerful methods to clarify the microscopic picture of complex biochemical and biophysical processes during gastrulation is to investigate them *in vitro*, when the contribution of different factors can be fully controlled and quantified.[11] Although it is clear that *in vitro* studies might not fully represent *in vivo* biological phenomena, they provide very useful information on the mechanisms and trends of cellular processes. However, earlier attempts to observe spatial patterning in embryonic stem cells were not successful.[12,13] The breakthrough came only recently in the study that utilized a geometric confinement of ESC colonies to trigger the self-organized pattern formation in the system.[11] In these experiments, embryonic stem cells were grown in disk-shape colonies of precisely controlled size and geometry. They were treated by Bone-Morphogenetic Protein 4 (BMP4) molecules to stimulate cell differentiation. As a result, three different types of cells starting from the edge of colonies were identified within 24 h after the treatment by signaling molecules.[11] One of the most surprising experimental observations is the appearance of an intrinsic length scale of the cell differentiation band, which is fixed and independent on the size of the colony.[11,14,15] It was also found that the patterning strongly depends on the reaction between BMP4 molecules and their inhibitors that are produced by the ESCs. In addition, these experiments suggest that the boundary of the colony and the leakage of molecular ingredients beyond the boundary are necessary for the pattern formation.[11]

These experimental studies clarified many aspects of complex processes that are taking place during the early stages of the biological development. It is known that spatial patterning during gastrulation is governed by several major biological signaling pathways.[4,5,19] Non-uniform profiles of signaling molecules, also called morphogens, stimulate different fates in embryonic cells at different spatial positions at different times.[17,18] However, these experiments also raised several important questions: Why is there the universal length scale for the spatial patterning? What is the molecular picture behind this phenomenon? How signaling molecules specifically influence the spatial pattern formation in ESCs? What is the role of geometric boundaries of the colony?

In this paper, we develop a minimalist computational model that allows us to analyze the processes that are taking place during gastrulation. Our idea is that the effect of signaling pathways can be modeled using reaction-diffusion processes, and the concentration profiles of major signaling molecules directly specify the fates of the embryonic cells. Using this theoretical approach, we are able to explain the appearance of universal length scale, which is independent of the system size, the role of the boundaries, and the contribution of

different signaling molecules in the spatial patterning. Thus, the developed theoretical framework provides physical-chemical explanations of complex processes during gastrulation.

II. THEORETICAL MODEL

Although there are several signaling biochemical pathways that are involved in the gastrulation processes, to simplify the analysis we concentrate only on the bone-morphogenetic proteins pathway. This is also the way ESCs were treated in recent experiments.[11] Our idea is to develop a minimalist theoretical approach that can explain experimental observations and provide a consistent physical-chemical picture of complex processes during gastrulation. It is known that each embryonic cell constantly produces molecules that are antagonists to BMP4 molecules.[16] Once released, these inhibitor species can reversibly bind to free BMP4 molecules, preventing them from interactions with other ESCs and other ingredients of signaling pathway. We assume that the fate of embryo cells is governed by the local concentration of BMP4 morphogens. Then to describe different cellular patterns, the concentration profiles of signaling molecules should be evaluated. To do so, we take into account the chemical reactions involving different components of the signaling pathway, the possible diffusion of signaling molecules inside the colony and leaking outside of the colony.

Let us consider a model presented in Fig. 1, in which embryonic stem cells are confined within a circular two-dimensional boundary with a diameter equal to $2R$, similar to the experiments of Warmflash *et al.*[11] In these experiments, cells are grown on tissue culture dishes coated with a special matrix material, and colonies are mostly single-layer structures, justifying our assumption of describing the system as two-dimensional. Each stem cell of diameter $h = 10\ \mu$m is represented by a node on a square lattice and it produces inhibitor (I) molecules with a rate Q. To simplify the analysis, the colonies are viewed as 2D square lattices of embryonic cells. For every colony size, the number of cells is fixed. At time zero, the entire colony is exposed to a large amount of uniformly distributed BMP4 molecules. An inhibitor molecule I can reversibly associate with BMP4, forming a compound

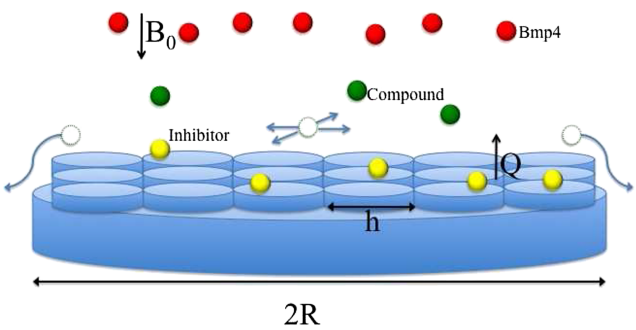

FIG. 1. A schematic view of the ESC colony exposed to BMP4 molecules. Each stem cell is represented by a node in two-dimensional square lattice, and it constantly produces inhibitor molecules, which reversibly react with free BMP4 molecules. Cells are bound to a special tissue culture matrix that supports their growth, and they are confined to a circular boundary from which the molecules can leak to outside of the system.

molecule (C), as described by

$$I + B \underset{k_b}{\overset{k_f}{\rightleftharpoons}} C, \tag{1}$$

where k_f and k_b are the forward and backward reaction rates, respectively, and B labels BMP4 molecules. It is assumed that all molecules have different diffusivities, and they could escape the colony through the edge of the circular boundary, see Fig. 1. The escape rates are k_I, k_B, and k_C for I, B, and C molecules, respectively. The temporal evolution of local molecular concentrations $[I]$, $[B]$, and $[C]$ (expressed as a number of molecules per unit area of the colony) are governed by the corresponding reaction-diffusion equations. More specifically, for the inhibitor molecules at any arbitrary embryonic cell, it can be written as

$$\frac{\partial [I]}{\partial t} = D_I \nabla^2 [I] - k_f [I][B] + k_b [C] + Q, \tag{2}$$

where D_I is the diffusion constant for inhibitor molecules. The physical meaning of this equation is the following: The local concentration of I molecules changes due to diffusion [the first term on the right side of Eq. (2)], it decreases due to binding to the BMP4 molecules [the second term on the right side of Eq. (2)], it increases due to reverse reaction of breaking the compound C [the third term on the right side of Eq. (2)], and it also increases due to the local production with the rate Q [the fourth term on the right side of Eq. (2)]. At the colony edge, we have the following boundary conditions for the inhibitor molecules:

$$D_I \nabla [I]\ |_{r=R} = -k_I [I]\ |_{r=R}. \tag{3}$$

These boundary conditions are justified by the fact that the chemical molecules produced by cells can diffuse beyond the boundaries of colonies, as observed in experiments.[11] Note also that, to simplify the analysis, we assume that the production of inhibitor molecules is independent of the signaling levels.

Similar reaction-diffusion equations can be written for other components of signaling pathway. For BMP4 molecules, it can be shown that

$$\frac{\partial [B]}{\partial t} = D_B \nabla^2 [B] - k_f [I][B] + k_b [C], \tag{4}$$

with the boundary condition given by

$$D_B \nabla [B]\ |_{r=R} = -k_B [B]\ |_{r=R}. \tag{5}$$

For the C molecules, we have

$$\frac{\partial [C]}{\partial t} = D_C \nabla^2 [C] + k_f [I][B] - k_b [C], \tag{6}$$

with the boundary condition given by

$$D_C \nabla [C]\ |_{r=R} = -k_C [C]\ |_{r=R}. \tag{7}$$

In addition, we assume that initially ($t = 0$) the concentration of BMP4 molecules was equal to B_0, i.e., the ESC colony was treated to the total number of BMP4 molecules equal to $B_0 * \pi R^2$, and there was no production of B or C molecules in our system.

Because of the radial symmetry of colonies, it is convenient to consider radial concentrations of the signaling components,

$$b(r,t) = \int_0^{2\pi} [B](r,\theta;t)d\theta,$$
$$i(r,t) = \int_0^{2\pi} [I](r,\theta;t)d\theta, \quad (8)$$
$$c(r,t) = \int_0^{2\pi} [C](r,\theta;t)d\theta,$$

where $[B](r,\theta;t)$, $[I](r,\theta;t)$, and $[C](r,\theta;t)$ are concentrations of B, I, and C molecules, respectively, at time t at the cell located at the position (r,θ), using the polar coordinates with the origin at the center of the colony, see Fig. 1. The total number of signaling molecules in the system at time t can be found from

$$B_{tot}(t) = \int_0^R b(r,t)rdr,$$
$$I_{tot}(t) = \int_0^R i(r,t)rdr, \quad (9)$$
$$C_{tot}(t) = \int_0^R c(r,t)rdr.$$

The reaction-diffusion equations for molecular concentrations of various components can be solved on the lattice using Monte Carlo simulations via the Gillespie algorithm[21] for different system sizes and for different sets of parameters. Here we do not assume that the system is in the stationary state, and the temporal evolution of signaling molecule profiles is fully investigated. It should also be noted that Eqs. (2)–(7) could be analyzed by developing a corresponding continuum description. However, we chose not to follow this route for two reasons. First, there are nonlinear terms in Eqs. (2) and (4), which cannot be neglected, that complicate the analysis. Second, the size of the cells in experimental systems (h = 10 μm) was not much smaller than the size of the system and the size of the new pattern near the border of the colony,[11] and the discrete nature of the system might be important as we show below.

III. RESULTS AND DISCUSSIONS

Experimental investigations on the BMP morphogen gradients suggest that the diffusion rate of free BMP4 molecules is very restricted, i.e., D_B is probably very small compared with mobilities of other molecules participating in the process.[20] In this scenario, BMP4 molecules do not diffuse much in their free form but become mobile only via bonding with fast inhibitor molecules. To account for this possibility, we consider a simple limiting case, in which $D_B = k_B = 0$ while other components of the system diffuse freely and can leave the colony.

The reaction-diffusion model described in Eqs. (2)–(7) is analyzed using computer simulations for three different sizes of ESC colonies that were utilized in experiments:[11] for 250, 500, and 1000 μm in diameter, respectively. The results are presented in Figs. 2–4. Figure 2(a) shows the snapshot of the

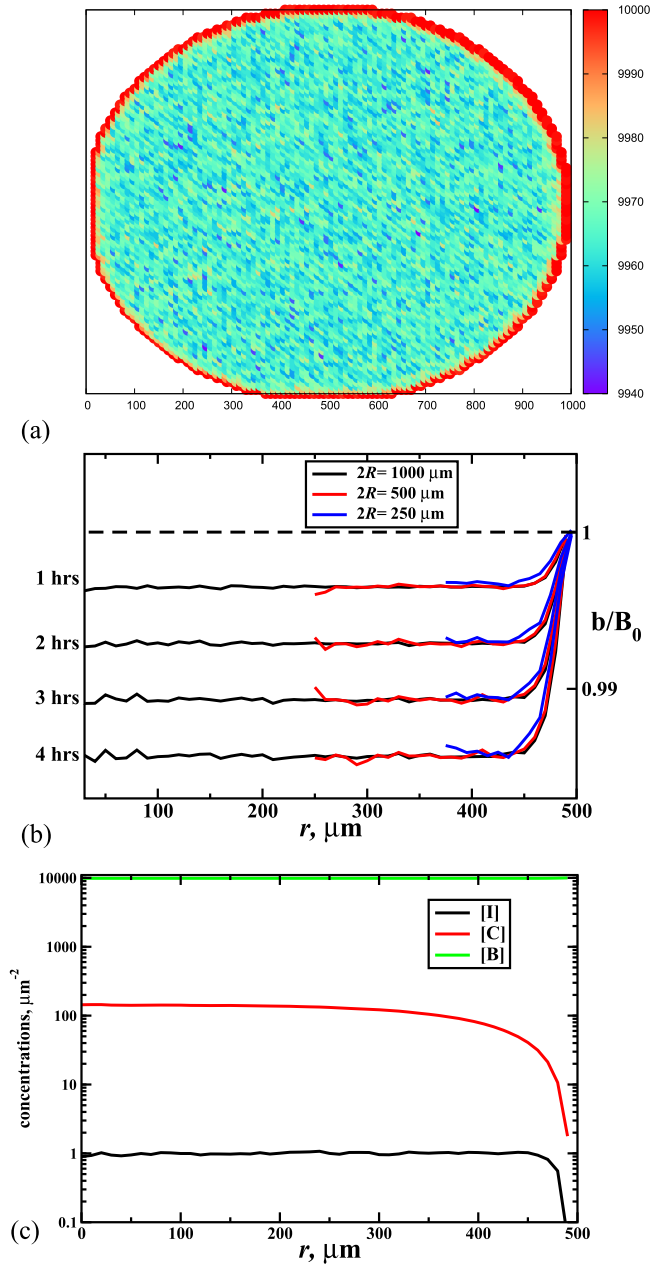

FIG. 2. Density profiles for signaling molecules with $D_B = k_B = 0$. (a) A top view snapshot of BMP4 molecular density 1 h after the exposure of the system of embryonic stem cells to BMP4 for the colony of size $2R = 1000\,\mu$m. Each point represents one stem cell. High/low BMP4 densities are shown in red/blue. The bar shows the number density of BMP4 molecules per each cell. (b) The formation of BMP4 morphogen gradient after 1, 2, 3, and 4 h for three different system sizes. Distances are indicated from the center of the colony. The lines for smaller system sizes are shifted to show their overlap at the border. The results are from single simulations in which each data point is a radially averaged value of densities within 3 min time interval. The concentration $[B]$ is scaled with a constant B_0, which corresponds to the initial concentration of BMP4 molecules. (c) Molecular concentrations of BMP4, inhibitor, and compound molecules 4 h after the exposure to BMP4. The following parameters were used for calculations: $D_I = D_C = 1\ \mu$m^2/s; $k_I = k_C = 10\ \mu$m/s; $k_f = 10^{-6}\ \mu$m^2/s; $k_b = 10^{-8}$ s^{-1}; $Q = 10^{-3}\ \mu$m^{-2} s^{-1}; and $B_0 = 10\,000\ \mu$m^{-2}.

concentration profile of BMP4 molecules 1 h after exposing the whole colony of ESC to the BMP4 signaling molecules with $[B] = B_0$. This morphogen gradient clearly shows two main regions. There is a low uniform density of BMP4 molecules in the center of the colony, while at the edge of the system (approximately 20-30 μm for this set of conditions), the concentration of signaling molecule is quite large, and it did not decrease much from the original concentration B_0. Although the concentration profiles change with time, the overall qualitative picture of two regions of signaling molecules remains the same, as one can see from Fig. 2(b) for different colony sizes. But there is one important conclusion from analyzing Fig. 2(b). There is a unique length scale that separates two regions of morphogen gradients, which is independent of the time and of the size of the system. In fact, when shifted toward the edge, density profiles perfectly overlap and the resulting differentiation bands are of the same width regardless of the system size [Fig. 2(b)]. Such bands are also visible in the top view of simulated colonies: see Fig. 2(a) where we show only one snapshot corresponding to the biggest colony. If one assumes that different concentrations of BMP4 stimulate different fates of ESCs, then our results remarkably reproduce the experimental observations in early embryonic spatial patterning.[11] The appearance of the same length scale can be also seen in the concentration profile of inhibitor molecules, as presented in Fig. 2(c). One should note here that the elevated level of BMP molecules is restricted to the colony edge, and thus it cannot pattern all cellular fates but only those close to the edge. This observation is consistent experimental results showing the importance of secondary signaling by Nodal to determine the fates of cells further away from the colony boundaries.[11]

To test the robustness of our theoretical predictions, we performed extensive number of computer simulations for three system sizes, as well as for different values of the diffusion rates, D_I and D_C, the removal rates k_I and k_C, and the reaction rates, k_f and k_b. In all these calculations, the parameter values span across several orders of magnitude, covering essentially all possible realistic values of dynamic and chemical kinetic properties of participating signaling molecules. Some of these tests are presented in Fig. 3. The normalized density of BMP4 molecules is not affected by variations in the diffusion constant D_C of the compound C by six orders of magnitude [Fig. 3(a)]. Similarly, the BMP4 morphogen gradient is robust with respect to changing the removal rate k_C by nine orders of magnitude [Fig. 3(b)]. In addition, varying the compound C breakage rate k_b does not modify the concentration profile of BMP4 molecules. Our calculations suggest that regardless of what values of parameters we take, the qualitative picture of two regions in the BMP4 concentration profile as a function of the distance from the center of the colony is always preserved. In the center of the colony, there is a region of uniformly low density, while the band near the edge of the colony has the larger concentration of BMP4 molecules. Surprisingly, our observations also indicate that the dynamics of the compound molecules C, which is determined by the parameters D_C, k_C, and k_b, do not affect the density profile of BMP4 even quantitatively. But varying other dynamic properties, such as D_I, k_I, and k_f, changes the relative fractions of two regimes in the

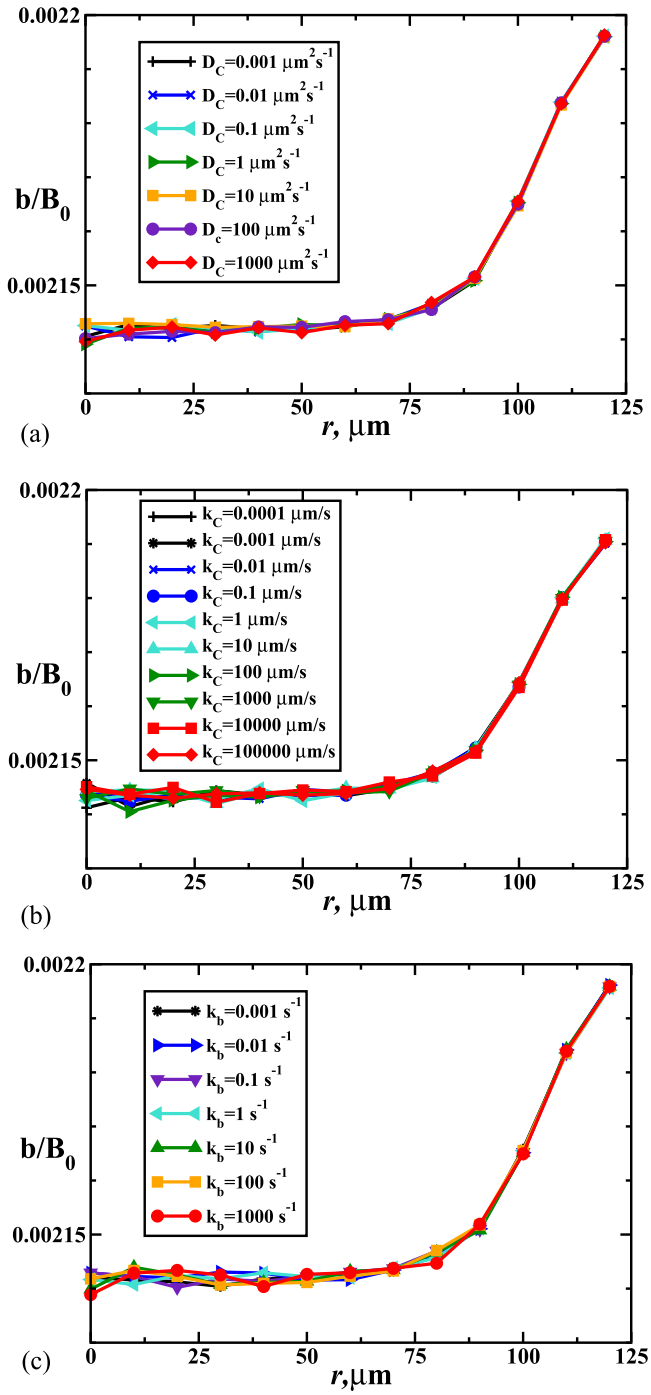

FIG. 3. Normalized concentration profiles of BMP4 molecules as a function of the distance from the center of the colony for varying system parameters. Each line shows the morphogen gradient 6 h after exposure to the signaling molecules. On each plot only one parameter is changed and the rest is kept constant. The size of the system is $2R = 250$ μm. (a) Varying the diffusion rate D_c; (b) varying the removal rate k_c; and (c) varying the breakage rate k_b. Parameters used for calculations are the same as in Fig. 2 except for varying D_c, k_c, and k_b, correspondingly.

morphogen gradient, without modifying the two-region structure.

One of our main results, which is also consistent with experimental observations, is the appearance of the universal length scale that divides the morphogen gradient of BMP4 molecules into two parts. To quantify this length, l_0, better, we consider $B_{tot}(t)$, which is the total amount of free BMP4

molecules in the colony at time t. Note that unlike B_0, $B_{tot}(t)$ is not a constant and changes with time. The time-dependent fraction of BMP4 molecules at the distance r from the origin is given by $b(r, t)/B_{tot}(t)$. Then we define the length l_0 as the length at which this fraction is independent of the time. The results are presented in Fig. 4(a). One can see that for the region between the edge of the colony and the length l_0, the relative fraction of BMP4 molecules increases, while for the center of the colony, the fraction decreases. This shows that l_0 is indeed the universal length scale, which is independent of the system size. We also found [see Fig. 4(b)] that this length scale is proportional to the parameter $(D_I/k_f B_0)^{0.5}$ which has a physical meaning of being proportional to the average distance that the inhibitor molecule diffuses in the system after the production when the concentration of BMP4 molecules is equal to B_0. This is because $k_f B_0$ is the effective rate of eliminating free inhibitor molecules via the chemical reaction. When this average length decreases to 10 μm, which is equal to the size of the embryonic cell in our computations, the universal length scale l_0 becomes independent of this length since inhibitor molecules are not able to diffuse beyond the cell where they were produced, see Fig. 4.

So far, computer simulations were done for the special case of zero diffusion of BMP4 molecules. Our method can be extended to relax this condition, and it can be shown that the qualitative picture of two regions in the concentration profile is still observed as long as $D_B < D_I$, and the diffusion of inhibitor molecules is not too fast for the fixed sizes of ESC colonies. Our calculations also show that the local production rate of the inhibitor molecules Q does not affect any of the results presented in this work.

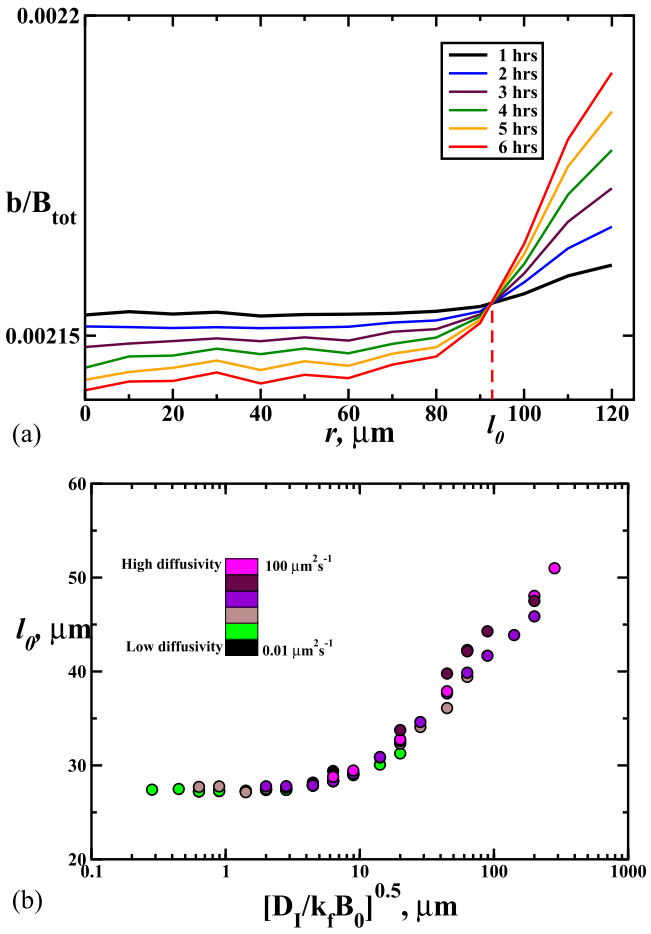

FIG. 4. (a) Time-dependent fraction of BMP4 molecules as a function of the distance from the center of the colony for different exposure times. The size of the system is $2R = 250\,\mu$m. (b) The dependence of the characteristic length scale on the parameter $(D_I/k_f B_0)^{0.5}$. Parameters used for calculations are the same as in Fig. 2, but with varying D_I and k_f in (b).

The following theoretical picture of the early spatial patterning in ESC is emerging from our theoretical calculations. As soon as the system is exposed to BMP4 molecules with the concentration B_0, ESCs start to produce inhibitor molecules that can react with them. The length $(D_I/k_f B_0)^{0.5}$ specifies the average distance that molecules I can move before being removed from the system via the reaction with BMP4. Because the inhibitor molecules can leave the system from the edge, this sets up the length scale of changing $[I]$ from the boundary concentrations to the bulk concentrations. As time proceeds, BMP4 molecules are consumed by inhibitor molecules everywhere in the system except the region of length $l_0 \approx (D_I/k_f B_0)^{0.5}$, where $[I]$ is already diminished, and the amount of compound molecules is also small, see Fig. 2(c). This situation is almost stationary as long as the amount of BMP4 molecules is large enough so that the existence of two regions in the morphogen gradients is not disturbed much. The important condition for separating the morphogen gradients in two regions is that BMP4 molecules diffuse much slower than the inhibitor molecules. These arguments explain the experimental observations that inhibitors to the BMP signaling pathway are necessary for the formation of different cellular patterns.[11] Our theoretical picture also emphasizes the important role of the boundaries since the length scale can be established only from the edge of the system, and this again agrees with experimental results.[11]

IV. SUMMARY AND CONCLUSIONS

We developed a theoretical approach to analyze complex processes taking place during gastrulation. More specifically, our theoretical method provides a molecular description of spatial patterning of embryonic stem cells during the early stages of biological development in animals. By taking into account the dynamic and chemical kinetic properties of signaling molecules of the BMP pathway, which is known to govern the fates of embryonic cells, a minimal reaction-diffusion model of the formation of morphogen gradients is constructed and analyzed using extensive Monte Carlo computer simulations. It is found that when the diffusion of BMP4 molecules is restricted, the concentration profiles of signaling molecules in the colony, originally exposed to BMP4 molecules, develop two regions. In the area close to the edge of the colony, the concentration of BMP4 molecules is quite large, while in the central part of the system, it is uniformly low. Our calculations indicate that the length scale that separates these two regions is a universal quantity that does not depend on the size of the ESC colonies. It is shown that this length scale is generally proportional to the average distance that free inhibitor molecules diffuse in the system, underlining the critical importance of the inhibitor

species in the process. The role of the leaking of signaling molecules from the colony is also discussed. Our theoretical calculations fully agree with experimental observations on the spatial patterning phenomena in ESCs, thus providing a consistent molecular picture of physical-chemical mechanisms of gastrulation.

Although our theoretical study is able to explain some features of the gastrulation processes, we should emphasize the very limited and approximate nature of our theoretical method that is trying to capture extremely complex biological phenomena. For example, during gastrulation, three different bands of embryonic cells appear, while our approach can only explain the differentiation into two groups. Clearly, more details of signaling pathways are needed to present a more realistic description of spatial pattern formation in the biological development. In addition, our theory completely neglects the cellular mobility and transformations, which might also strongly influence the gastrulation processes. In addition, we do not take into account the growth of cells: during the times considered in this work, cells will divide approximately 1-2 times, and the density in the constrained colony increases and becomes non-uniform. Thus, our theoretical findings must be viewed as the first step in developing more comprehensive theoretical models that will uncover the molecular mechanisms of gastrulation phenomena.

ACKNOWLEDGMENTS

This work was supported by the Welch Foundation (Grant No. C-1559), by the NSF (Grant Nos. CHE-1360979 and CHE-1664218), and by the Center for Theoretical Biological Physics sponsored by the NSF (Grant No. PHY-1427654). We also thank A. Warmflash for introducing us to this problem and for useful discussions and comments.

[1] A. Martinez-Arias and A. Stewart, *Molecular Principles of Animal Development* (Oxford University Press, New York, 2002).
[2] H. Lodish, A. Berk, C. A. Kaiser, M. Krieger, M. P. Scott, A. Bretscher, H. Ploegh, and P. Matsudaira, *Molecular Cell Biology*, 6th ed. (W. H. Freeman, New York, 2007).
[3] L. Wolpert, *Principles of Development* (Oxford University Press, New York, 1998).
[4] S. J. Arnold and E. J. Robertson, Nat. Rev. Mol. Cell Biol. **10**, 91 (2009).
[5] L. Solnica-Krezel and D. S. Sepich, Annu. Rev. Cell Dev. Biol. **28**, 687 (2012).
[6] Y. Nakaya and G. Sheng, Dev., Growth Differ. **50**, 755 (2008).
[7] R.-H. Xu, R. M. Peck, D. S. Li, X. Feng, T. Ludwig, and J. A. Thomson, Nat. Methods **2**, 185 (2005).
[8] G. Keller, Genes Dev. **19**, 1129–1155 (2005).
[9] A. M. B. Tadeu and V. Horsley, Development **140**, 3777–3786 (2013).
[10] V. Tabar and L. Studer, Nat. Rev. Genet. **15**, 82–92 (2014).
[11] A. Warmflash, B. Sorre, F. Etoc, E. D. Siggia, and A. H. Brivanlou, Nat. Methods **11**, 847 (2014).
[12] M. Drukker, C. Tang, R. Ardehali, Y. Rinkevich, J. Seita, A. S. Lee, A. R. Mosley, I. L. Weissman, and Y. Soen, Nat. Biotechnol. **30**, 531–542 (2012).
[13] T. A. Blauwkamp, S. Nigam, R. Ardehali, I. L. Weissman, and R. Nusse, Nat. Commun. **3**, 1070 (2012).
[14] K. A. Rosowski, A. F. Mertz, S. Norcross, E. R. Dufresne, and V. Horsley, Sci. Rep. **5**, 1428 (2015).
[15] F. Etoc, J. Metzger, A. Ruzo, C. Kirst, A. Yoney, M. Z. Ozair, A. H. Brivanlou, and E. D. Siggia, Dev. Cell **39**, 302 (2016).
[16] R. Peerani, B. M. Rao, C. Bauwens, T. Yin, G. A. Wood, A. Nagy, E. Kumacheva, and P. W. Zandstra, EMBO J. **26**, 4744 (2007).
[17] H. Teimouri and A. B. Kolomeisky, J. Phys. A: Math. Theor. **49**, 483001 (2016).
[18] A. Porcher and N. Dostatni, Curr. Biol. **20**, R249 (2010).
[19] D. M. Umulis and H. G. Othmer, Development **140**(24), 4830 (2013).
[20] A. Eldar, R. Dorfman, D. Weiss, H. Ashe, B. Shilo, and N. Barkai, Nature **419**, 304 (2002).
[21] D. Gillespie, J. Phys. Chem. **81**, 2340 (1977).